Analysis of Urban Surface Biophysical Descriptors and Land Surface Temperature Variations in Jimeta City, Nigeria

Ambrose A. Zemba

GJHSS Classification (FOR)
040302, 040307, 040606 & 040608

Abstract: **Land-use and land-cover (LULC) data are often employed for simple correlation analyses between LULC types and their thermal signatures in the studies of land surface temperature (LST) using remote sensing. This tends to slow down the development of remote sensing of land surface temperature. Hence, there is need for methodological shift to quantitative surface descriptors. Development of quantitative surface descriptors could improve our capabilities for modeling urban thermal landscapes and advance urban climate research. This study therefore adopted an analytical procedure based on a spectral derivation model for characterizing and quantifying the urban landscape in Jimeta, Nigeria. A Landsat Enhanced Thematic Mapper Plus (ETM+) image of the study area, acquired on 16 November 2008, was spectrally modeled into three fraction endmembers namely, green vegetation, soil, and impervious surface. A hybrid classification procedure was developed to classify the fraction images into six land-use and land-cover classes. Next, pixel-based LST measurements were related to urban surface biophysical descriptors derived from spectral mixture analysis (SMA). Correlation analyses were conducted to investigate land-cover based relationships between LST and impervious surface and green vegetation fractions for an analysis of the causes of LST variations. Results indicate that fraction images derived from SMA were effective for quantifying the urban morphology and for providing reliable measurements of biophysical variables such as vegetation abundance, soil and impervious surface. An examination of LST variations within the city and their relations with the composition of LULC types, biophysical descriptors, and other relevant spatial data shows that LST possessed a weak relation with the LULC compositions than with other variables (including urban biophysical descriptors, remote sensing biophysical variables, GIS-based impervious surface variables, and population density).**

Key words: Land surface temperature, urban surface biophysical descriptors, Land use, Land cover

I. Introduction

Because the receipt and loss of radiation of urban surfaces correspond closely to the distribution of land-use and land-cover (LULC) characteristics, there has always been a tendency to use thematic LULC data, not quantitative surface descriptors, to describe urban thermal landscape. This has slowed down the development of remote sensing of land surface temperatures (LST) and thus surface temperature heat islands (Voogt and Oke, 2003). However, Clapham (2003) suggested using of a continuum-based classification for satellite imagery, which aims to provide continous data for the functional classes. The idea of continuum-based classification has long been pursued in urban landscape analysis. One of the major contributions is Ridd's (1995) vegetation-impervious surface-soil (V-I-S) model for characterizing urban environments. This model assumes that urban land-cover is a linear combination of three biophysical components: vegetation, impervious surface, and soil and has recently been successfully implemented by using the technique of spectral mixture analysis (Madhavan et al, 2001; Rasheed et al, 2001; Small, 2001; Phinn et al, 2002; Wu and Murray, 2003; and Lu and Weng, 2004). The Ridd model provides the potential for a link between remote sensing-derived urban biophysical components and LST, and may be applied to establish parameters for describing urban construction materials and fabrics to improve our understanding of urban surface energy budget and heat islands.

The focus of this research is placed on the application of a methodology to examine the interplay between LST and urban morphology. A Landsat ETM+ image of 2008 that covers the City of Jimeta, Nigeria was used in conjunction with other types of spatial data for the analysis. The specific objectives were twofold: First, to employ spectral mixture modeling to derive urban surface biophysical attributes, and to apply spectrally unmixed results to characterize the urban landscape and secondly, to analyze the causes of LST variations, which were derived from Landsat thermal infrared data by linking LST with remotely sensed urban surface biophysical descriptors.

II. Study Area

Jimeta, a twin city to Yola town, is the capital of Yola North Local Government and Adamawa State of Nigeria. The city is located at the bank of River Benue, between latitude 9^0 10' to 9^0 15'N and longitude 12^0 11' to 12^0 17'E. The area has a Sudan type of vegetation and a tropical climate marked by wet and dry seasons. The minimum temperature recorded is about 15 ^{0}C and a maximum of about 40 ^{0}C.

The city has been experiencing an increasing population explosion since it assumed a status of Adamawa State capital in 1976. Like any other Nigerian cities, Jimeta comprises of so many land use types ranging from institutional, commercial, and residential. The city is clearly stratified in terms of population densities (Ilesanmi, 1999).

About- Geography Department, Federal University of Technology, P.M.B. 2076, YolaContact no:+234 806 913 7174, +234 808 181 4644 Email:aazemba@yahoo.com

These are low, medium and high density areas. The low density areas are well planned units where government officials reside while medium and high density areas are made up of common people with little or unplanned streets and buildings.

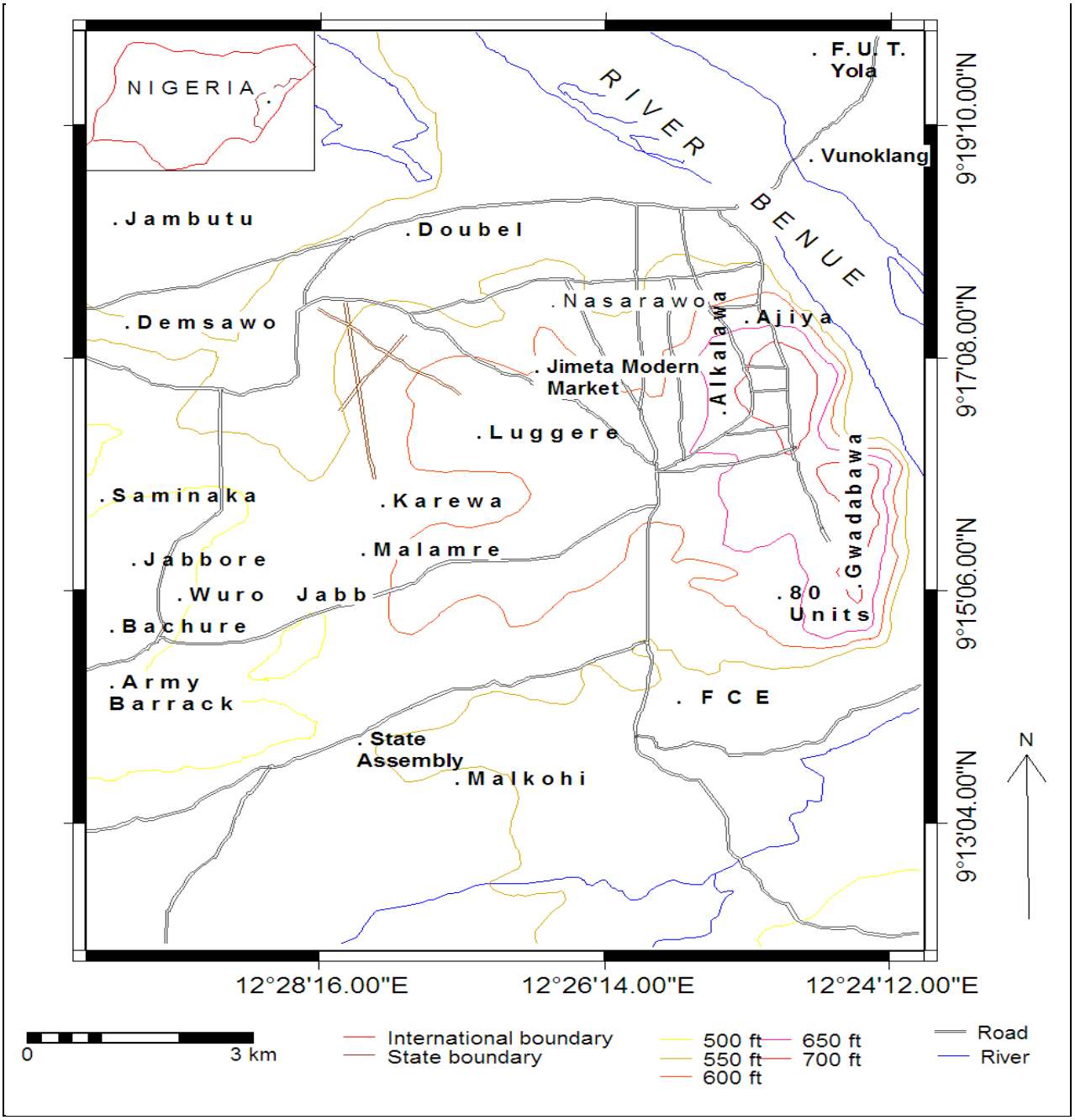

In recent times, Jimeta has risen as the premier commercial, industrial and transportation urban area of the northeastern Nigeria. The rapid growth of Jimeta, particularly within the past 30 years, has made it one of the fastest growing metropolitan areas in Nigeria. For instance, the population of Jimeta increased significantly by 69% between 1973 and 1991 and 58% between 1991 and 2006 (NPC 2006). Concomitant with this high rate of population growth has been an explosive growth in retail, educational, commercial and administrative services within the area. This has resulted

in tremendous land cover change dynamics within the metropolitan region, wherein urbanization has consumed vast acreages of land adjacent to the city proper and has pushed the urban fringe farther away from the original Jimeta urban core. An enormous transition of land from forest and agriculture to urban land uses has occurred in the area, the extent of which needs to be investigated for the sake of planning for the ever growing population.

III. Methods

1. *Pre-processing of image*

Landsat 7-Enhanced Thematic Mapper Plus (ETM+) image with path/row of 185/54 dated 16 November 2008 was used in this research. The acquisition date has a highly clear atmospheric condition, and the image was acquired through the USGS Earth Resources Observation Systems Data Center, which has corrected radiometric and geometrical distortions of the image to a quality level of 1G before delivery. The major pre-processing on the image had to do with scan-line-off correction. The image was further rectified to a common Universal Traverse Mercator coordinate system based on 1:50, 000 scale topographic maps, and was resampled using the nearest neighbor algorithm with a pixel size of 30 m by 30 m for all bands including the thermal band.

2. *Spectral mixture analysis*

Spectral mixture analysis was employed to estimate endmember fractions in the images. Endmembers are recognizable land-cover materials that have homogeneous spectral properties all over the image. Spectral mixture analysis assumes that the spectrum measured by a sensor is a linear combination of the spectra of all components within the pixel (Adams et al, 1995). The mathematical model of linear spectral mixture analysis is expressed as

$$R_i = \sum_{k=}^{n} f_k R_{ik} + ER_i \text{ Where,} \qquad (1)$$

i = 1, ... m (number of spectral bands),
k = 1, ... n (number of end members)
R_i = Spectral reflectance of band i of a pixel which contains one or more endmembers;
f_k = Proportion or fraction of end member k within the pixel;
R_{ik} = Known spectral reflectance of end member k within the pixel on band i; and
ER_i = Error for band i or remainder between measured and modeled DN (band residuals).

Estimation of endmembers was done using reference endmember fractions i.e. the laboratory spectra of the target materials in Erdas imagine software.

3. *Estimation of impervious surface*

In this research, reference endmembers was applied. ERDAS Imagine GIS software has a collection of spectra libraries, from where the spectra that represent the materials used as endmembers (soil, vegetation and impervious surface) were selected.

4. *Land-use and Land-cover classification*

The maximum likelihood classification algorithm was applied to classify the fraction image into ten classes. A distance threshold was selected for each class and was determined by examining interactively the histogram of each class in the distance image. Pixels with a distance value greater than the threshold were assigned a class value of zero in thematic image. A distance tree classifier was then applied to reclassify these pixels. The parameters required by the distance tree classifier were identified based on the mean and standard deviation from the sample points of each class. Finally, the accuracy of the classified image was checked with a stratified random sampling method against the reference data of 50 samples collected from a large-scale 2006 aerial photograph of the study area. Six land use/cover types were identified, including (i) built-up land (ii) bare surface (iii) natural vegetation or forest (iv) Marshy land (v) croplands and (vi) water bodies. An overall accuracy of 88% and a Kappa index of 0.84 were determined.

2. *Estimation of Land Surface Temperature (LST)*

The Landsat TM and ETM+ thermal bands have different gain and offset values. Therefore, for the calculation of their radiance values, different formulas are used. In this study, for the calculation of radiance the formula in equation (2) was used:

$$\text{Radiance} = ((L_{MAX} - L_{MIN}) / (DN_{MAX} - DN_{MIN})) * (DN - DN_{MIN}) + L_{MIN} \quad \text{where:} \qquad (2)$$

For band 6L	and	For band 6H
L_{MAX} = 17.04		L_{MAX} = 12.65
L_{MIN} = 0.0		L_{MIN} = 3.2
DN_{MAX} = 255		DN_{MAX} = 255
DN_{MIN} = 1		DN_{MIN} = 1

The values for all these parameters were obtained from the data header files.

After the calculation of the radiance values, the temperature values were derived using the inverse of Planck function (equation 3), thus:

$$T_{(^0C)} = \left[\frac{K_2}{Ln\{K_1 / CV_R + 1\}} \right] - 273, \quad (3)$$

Where:

$T_{(^0C)}$ = *Temperature in Degrees Celsius*
CV_R = *Cell (pixel) value as radiance*
K_1 = *607.76 (for TM) or 666.09 (for ETM and ETM+) in* $mW\ cm^{-2}\ sr^{-1}\ \mu m^{-1}$
K_2 = *1260.56 (for TM) or 1282.71 (forETM and ETM+) in Kelvin*

All the temperature derivations were modeled using a Model Maker in Erdas Imagine software. In examining the spatial relationship between land use/cover types and the surface energy response as measured by surface temperature, a classified image was overlaid to the surface temperature images.

IV. Results

Urban Surface Biophysical Descriptors

Fig 2 shows the three fraction images derived. This consists of Green vegetation, soil, and impervious surface fractions. Pixel values of these fraction images represent areal proportions of each biophysical descriptor within a pixel. Green vegetation fraction image showed a large dark area (low values) at the centre of the study area that corresponds to the central business district of the city. Bright areas of high green vegetation values are found in the surrounding areas. Though, various types of crops were at their maturity stage, the green vegetation fraction images in the northwestern to southwestern parts of the city were still conspicuous as evidenced by medium gray to dark tone. Column 3 of Table 1 displays green vegetation fraction values by land cover types. Forest/sparse trees (including natural/planted trees, bushes and grasses) apparently had the highest green vegetation fraction values (0.715). In contrast, built-up lands displayed the lowest green vegetation values (0.119).

Little vegetation amount was also found in water bodies as indicated by the green vegetation fraction value (0.161). Bare surfaces or exposed soils, natural vegetated lands and cultivated or croplands put together yielded an intermediate green vegetation fraction values around 0.25. Bare surfaces green vegetation standard deviation was slightly lower in value than that of cultivated land. Cultivated land standard deviation was the highest (0.33), suggesting that cultivated land may be characterized by various amounts of vegetation coverage. The least value of standard deviation for green vegetation was recorded in forest areas indicating that a variation in the amount of vegetation cover is minimal.

The percentage of land covered by impervious surfaces may vary significantly with land use-land cover categories and sub-categories. This study reveals a substantially different estimate for each land use-land cover types. For example, a negative impervious

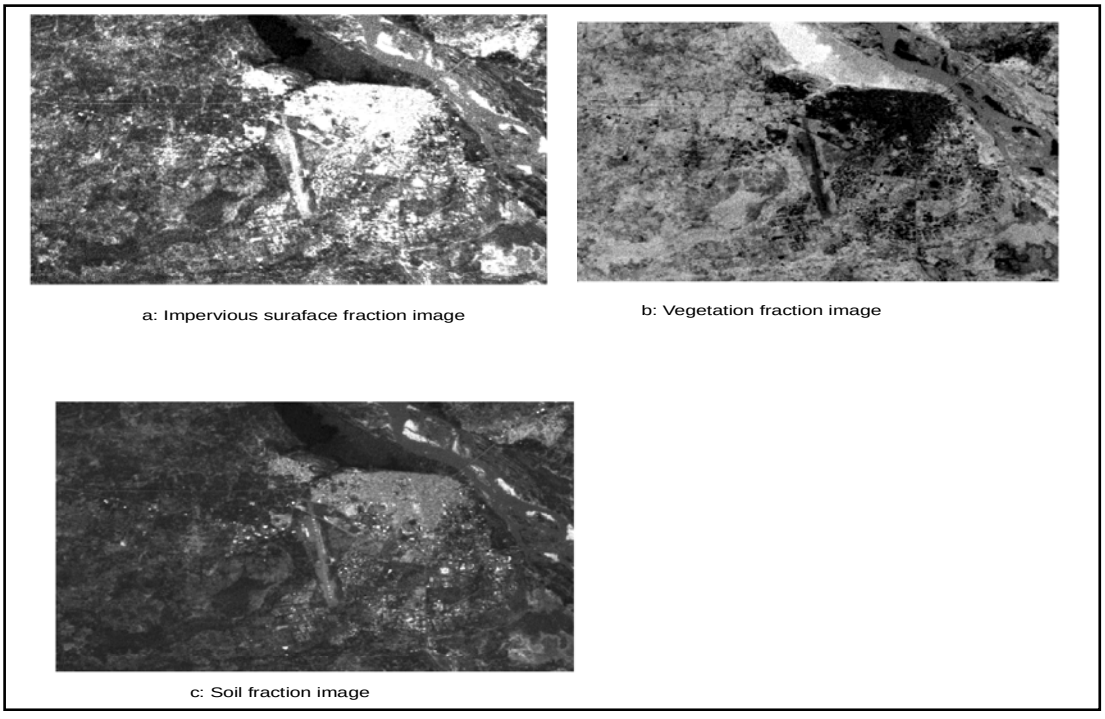

a: Impervious suraface fraction image

b: Vegetation fraction image

c: Soil fraction image

Fig 2: Fraction images derived from spectral mixture analysis of the landsat ETM+ 2008 image

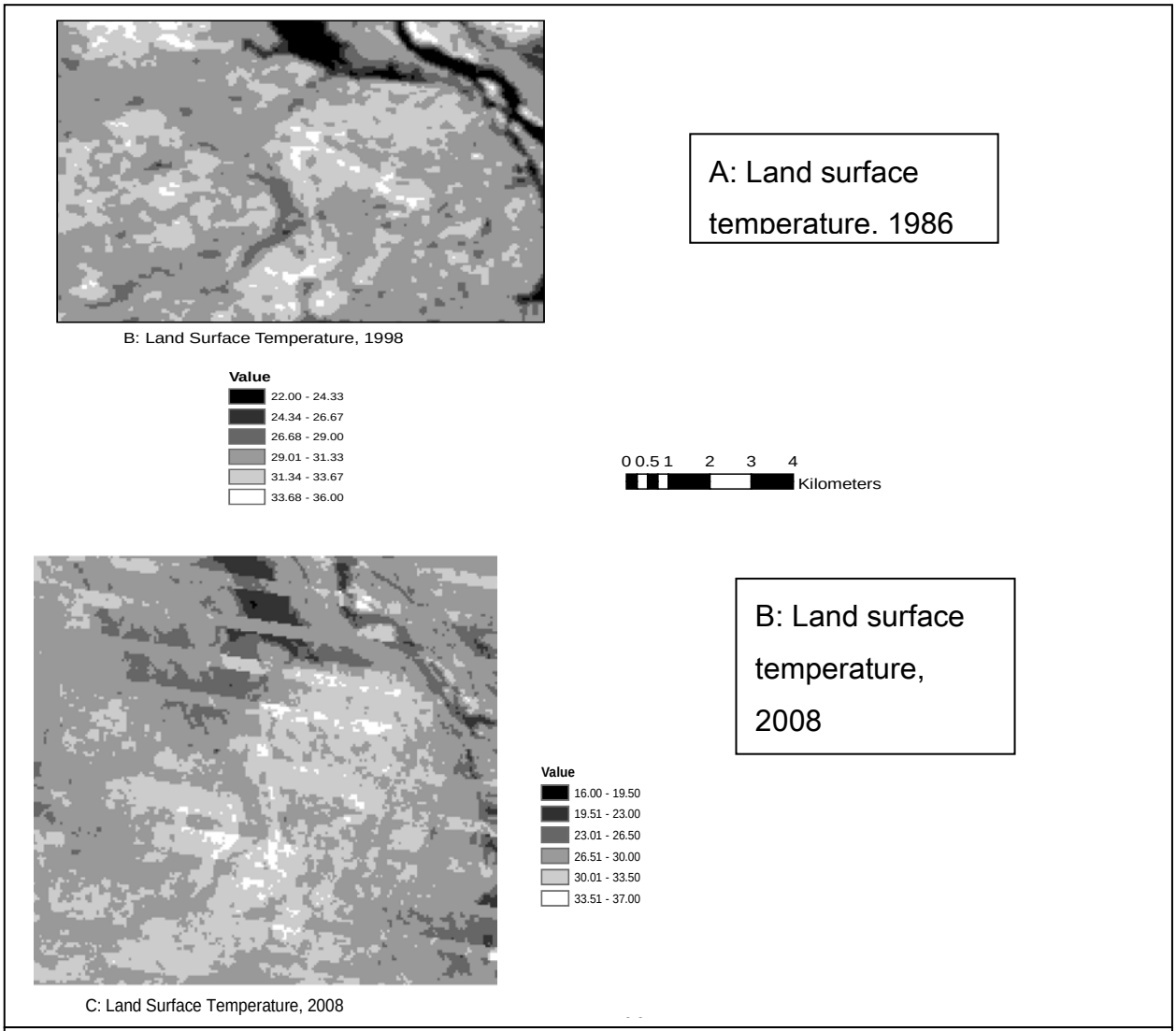

Fig 3: Land surface temperature variation in Jimeta in 1986 and 2008

Table 1: Descriptive Statistics of Biophysical Parameters of the Land Cover Types

Land Use & land cover	Mean LST in 2008 (^{0}C)	Mean Vegetation	Mean Impervious surface	Mean soil fraction
Built-up lands	36.85 (3.10)	0.119 (0.140)	0.491 (0.226)	0.101 (0.234)
Bare soils	32.85 (1.94)	0.276 (0.155)	0.254 (0.098)	0.147 (0.144)
Croplands	28.85 (1.56)	0.248 (0.333)	0.129 (0.045)	0.333 (0.252)
Marshy lands	27.85 (1.83)	0.258 (0.151)	0.138 (0.097)	0.373 (0.184)
Forest/bushy lands	26.85 (1.37)	0.715 (0.104)	0.057 (0.030)	0.01 (0.077)
Water	23.85 (0.43)	0.161 (0.178)	-0.029 (0.090)	-0.109 (0.156)

Source: Derived from Landsat ETM+ Image. Values in brackets refer to standard deviations

Results are displayed in the last two columns of Table 2. For all land use and land cover types, land surface temperature values were negatively correlated with green vegetation fraction values, but were positively correlated with impervious fraction values. The strongest negative correlation existed between land surface temperature and green vegetation fraction values in croplands (-0.7538) and forest (natural vegetation) (-0.7343). The correlation coefficient values dropped slightly for bare surface (-0.6763) and residential lands (-0.6559), with a sharp decrease for marshy lands. The least correlation was found in water (-0.2416). On the other hand, the strongest positive correlation between land surface temperature and impervious fraction values was found in crop lands (0.5558), followed by bare surfaces (0.5373). The weakest correlations (0.3267 and 0.3538) were observed in thick vegetation areas and water respectively.

Table 2: Statistics of the Biophysical Descriptors by Land use-land cover types, and their Correlations with land surface temperature (significant at 0.05 level)

Land Use-land cover Type	Mean LST	Mean Vegetation	Mean Impervious surface	LST/Vegetation Fraction	LST/Impervious surface
Built-up lands	39.85 (3.10)	0.119 (0.140)	0.491 (0.226)	- 0.6559	0.5254
Bare surface	32.85 (1.94)	0.276 (0.155)	0.254 (0.098)	- 0.6763	0.5373
Croplands	28.85 (1.56)	0.248 (0.333)	0.129 (0.045)	- 0.7538	0.5558
Marshy lands	27.85 (1.83)	0.258 (0.151)	0.138 (0.097)	- 0.4105	0.5290
Natural vegetation	26.85 (1.37)	0.715 (0.104)	0.057 (0.030)	- 0.7343	0.3267
Water	23.85 (0.43)	0.161 (0.178)	-0.029 (0.090)	- 0.2416	0.3538

Source: Derived from Landsat ETM+ Image (2008). Values in brackets are standard deviation

V. Conclusion

The use of thermal land use-land cover data is reported to have slowed down the development of remote sensing of land surface temperature and thus surface temperature heat island (Voogt and Oke, 2003). Hence, there has been a call to develop and apply quantitative surface descriptors to describe urban thermal landscapes in remote sensing studies. To make this happen, remote sensing techniques must enable parsimonious separation of urban land use/cover types into values directly related to their scale and signature (Phinn et al, 2002). This study has demonstrated that spectral mixture analysis (SMA), based on the V-I-S model, can provide a physically based solution for characterizing and quantifying urban landscape compositions, and that SMA-derived fraction estimates can be used as reliable urban surface biophysical descriptors. As a comparison, the study has examined the relationship between land surface temperature (LST) values and the compositions of LULC types within the city, as well as the relationships between LST and the urban biophysical descriptors derived from SMA, and other relevant spatial data. Results indicate that LST possessed a stronger relationship with these variables than the LULC compositions.

The study also revealed that SMA provides a suitable model to decompose the spectral mixtures of L-resolution data such as Landsat TM/ETM+. The scene elements in the L-resolution data are smaller than the resolution cell of the sensor, and are therefore not detectable. Thus, a more realistic representation and quantification of urban surfaces are possible, in comparison to that provided by assignment of a single dominant class to every pixel by statistical models. With the availability of multi-temporal satellite images, stable and reliable fraction estimates derived from SMA may be more efficient for a LULC change detection than traditional pixel-by-pixel comparison methods, because the fractional characteristics of LULC types at one date are comparable with other dates of fraction images. Fraction images may also be translated into significant environmental variables such as impervious surface and vegetation abundance. By relating LST to changing fraction constituency over time with urban growth, the effect of urbanization on LST may be examined.

VI. References

1) Adams, J. B., Sabol, D. E., Kapos, V., Filho, R. A., Roberts, D. A., Smith, M. O. & Gillespie, A. R. (1995) Classification of multispectral images based on fractions of endmembers: Application to land cover changes in the Brazilian Amazon. *Remote sensing of Environment, 52:137-154.*

2) Clapham, W.B. (2003) Continuum-based classification or remotely sensed imagery to describe urban sprawl on a watershed scale. *Remote Sens Environs 86:322-340.*

3) Ilesanmi, F.A. (1999) Urban Settlements In Adebayo, A.A. and Tukur, A.L. (eds) Adamawa State in Maps, Department of Geography, FUTY and Paraclete Publishers, Yola.

4) Lu, D. and Weng, Q. (2004) Spectral Mixture Analysis of the Urban Landscapes in Indianapolis with Landsat ETM+. *Photogrammetric Engineering & Remote Sensing, 70, 1053-1062.*

5) Madhavan, B.B., Kubo, S., Kurisaki, N. and Sivakumar, T.V.I.N. (2001) Appraising the Anatomy and Spatial Growth of the Bangkok Metropolitan Area Using a Vegetation-Impervious surface-Soil Model through Remote Sensing,

International Journal of Remote Sensing, 22:789-806

6) National Population Commission (NPC, 2006) Details of the breakdown of the national and state provisional population totals 2006 census.

7) Phinn, S., Stanford, M., Scarth, P., Murray, A. T. & Shyy, P. T. (2002) Monitoring the composition of urban environments based on the vegetation-impervious surface-soil (VIS) model by subpixel analysis techniques. *International Journal of Remote Sensing 23:4131-4153.*

8) Rasheed, T., Weeks, J. R., Gadalla, M. S. & Hill, A. G. (2001) Revealing the autonomy of cities through spectral mixture analysis of multispectral satellite imagery: A case study of the Greater Cairo region, Egypt, *Geocarto International 16, 5-15.*

9) Ridd, M.K. (1995) Exploring a V-I-S (vegetation-impervious surface-soil) model for urban ecosystem analysis through remote sensing: Comparative anatomy for cities. *International Journal of Remote Sensing* 16: 2165- 2185.

10) Small, C. (2001) Estimation of urban vegetation abundance by spectral mixture analysis, *International Journal of Remote Sensing, 22:1305-1354.*

11) Voogt, J.A. & Oke, T.R. (2003) Thermal Remote Sensing of Urban Climates. *Remote Sensing of environment, 86, 370-384*

12) Weng, Q. (2001) A Remote Sensing-GIS Evaluation of Urban Expansion & Its Impact on Surface Temperature in the Zhujiang Delta, China. *International Journal of Remote Sensing, 22 1999-2014.*

13) Wu, C. & Murray, A.T. (2003) Estimating Impervious Surface Distribution by Spectral Mixture Analysis. *Remote Sensing of Environment, 84, 493-505.*